ACS APPLIED MATERIALS & INTERFACES

Research Article

www.acsami.org

Air Ambient-Operated pNIPAM-Based Flexible Actuators Stimulated by Human Body Temperature and Sunlight

Yuki Yamamoto, Kenichiro Kanao, Takayuki Arie, Seiji Akita, and Kuniharu Takei*

Department of Physics and Electronics, Osaka Prefecture University, Sakai, Osaka 599-8531, Japan

Supporting Information

ABSTRACT: Harnessing a natural power source such as the human body temperature or sunlight should realize ultimate low-power devices. In particular, macroscale and flexible actuators that do not require an artificial power source have tremendous potential. Here we propose and demonstrate electrically powerless polymer-based actuators operated at ambient conditions using a packaging technique in which the stimulating power source is produced by heat from the human body or sunlight. The actuating angle, force, and reliability are discussed as functions of temperature and exposure to sunlight. Furthermore, a wearable device platform and a smart curtain actuated by the temperature of human skin and sunlight, respectively, are demonstrated as the first proof-of-concepts. These nature-powered actuators should realize a new class of ultimate low-power devices.

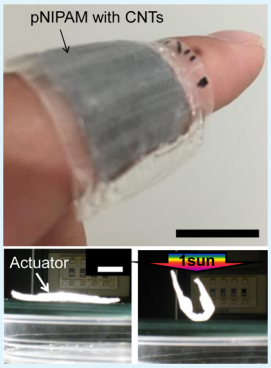

KEYWORDS: *actuators, pNIPAM, wearable devices, carbon nanotubes, ambient operations*

INTRODUCTION

Natural energy conversion into mechanical deformation represents electrically powerless devices for future ultimate low-power electronics, leading to green environments. Possible power sources for actuators that change shape or move include heat from the human body, sunlight, etc. For example, if a flexible/stretchable substrate could wrap around a human wrist or a finger by just placing it on the body due to the natural body temperature, it would be useful for wearable electronics. Another application is a smart curtain that opens and closes using sunlight.[1]

Several thermal/light-responsive actuators without an external electrical power source have been reported using polymer materials and nanomaterials such as carbon nanotubes (CNTs)[1,2] and graphene.[3−6] Nanocarbon materials that absorb light (especially infrared light) and convert it into heat[7] have realized actuation of a bilayer structure of nanocarbon (i.e., CNTs or graphene) on a flexible substrate in ambient air under infrared light.[1−3,5,6] This advance allows powerless actuators to create green energy devices. In the case of polymer materials, ultraviolet (UV) light,[8−11] strong laser light,[12,13] or another stimulus generated using an artificial power source[14,15] is often necessary.

Previously, poly(*N*-isopropylacrylamide) (pNIPAM) has been proposed as a thermal responsive actuator.[16] pNIPAM has a low critical solution temperature (LCST) of ∼32 °C.[17,18] Above the LCST (i.e., >32 °C), pNIPAM begins to desorp water from itself, causing it to shrink. Since pNIPAM is a reversible material at the LCST, pNIPAM absorbs water <32 °C, restoring its original shape. This behavior can be applied to an actuator, which must be operated in water.[16−18] Because the LCST ≈ 32 °C, pNIPAM has potential as a wearable device that can be wrapped around the body using the temperature of human skin if it can be operated in ambient air. In addition, if nanocarbons such as CNTs can be added into a pNIPAM film, the light absorption effect can be utilized to actuate it via sunlight.

In this study, we demonstrate a thermally and optically responsive actuator using pNIPAM with a packaging method that allows a pNIPAM actuator to be operated in ambient air. The technique is simple, but the approach using a packaging method for a flexible device should realize a next-generation structure that combines solid, vapor, and liquid states of materials for electronic devices. In fact, some approaches have recently utilized liquids in electrical devices.[19,20] By operating a pNIPAM actuator in air, the temperature dependence and actuation force are experimentally studied with and without CNTs. In addition, the light responsiveness using a solar simulator with 100 mW/cm^2 (one sun) is employed in a smart curtain application, which has potential for the robotic joints.

EXPERIMENTAL SECTION

The following steps were used to fabricate a packaged thermally and optically responsive pNIPAM actuator (Figure 1a). First, a 38 μm thick polyethylene terephthalate (PET) film was patterned to form line trenches (∼80 μm wide and 13 mm long) to support bending and the holes (∼150-μm diameter) to improve adhesion between PET and pNIPAM by a laser cutting tool (VLS2.30, Universal Laser Systems). Without having the adhesion holes, pNIPAM film does not adhere

Received: March 23, 2015
Accepted: May 4, 2015
Published: May 4, 2015

DOI: 10.1021/acsami.5b02544
ACS Appl. Mater. Interfaces 2015, 7, 11002−11006

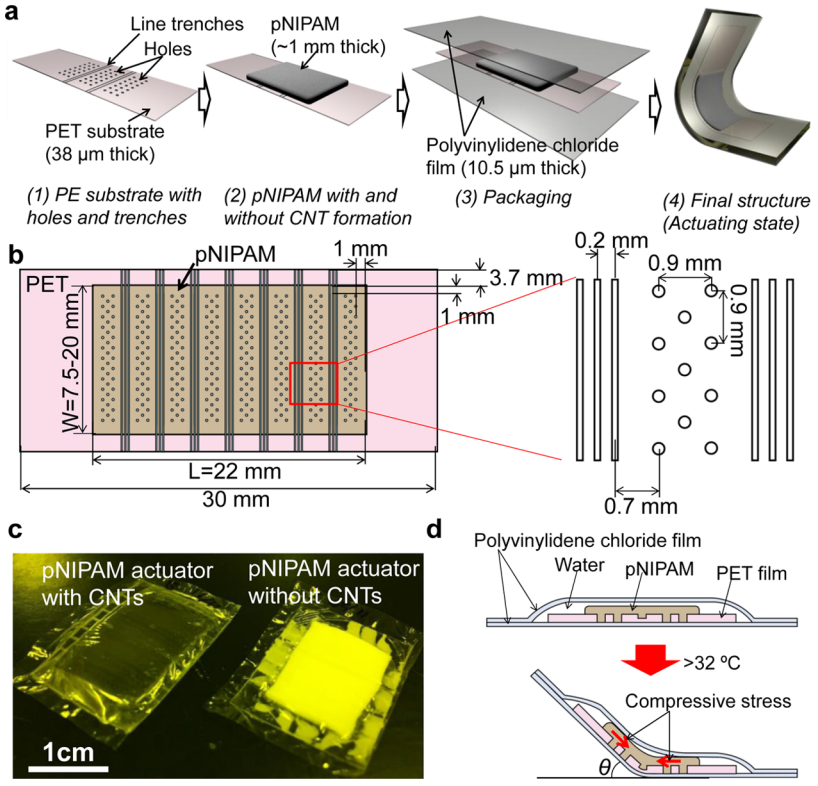

Figure 1. Packaged pNIPAM actuator. Schematics of (a) the fabrication process and (b) detailed design with line trenches and holes. (c) Photos of the fabricated pNIPAM actuator with and without CNTs. (d) Schematic of the actuation mechanism by shrinking pNIPAM and the definition of the bending angle θ.

well to the PET film, so that it cannot work as a pNIPAM/PET bilayer actuation material. Figure 1b depicts the detailed design. Then a pNIPAM solution was prepared by mixing the NIPAM powder (Wako Chemical Industries), *N*,*N*′-methylenebis(acrylamide) as a cross-linker (Tokyo Chemical Industry), 2,2′-diethoxyacetophenone as a photo-initiator (Sigma-Aldrich), and deionized water with a weight ratio of 300:9.25:2.5:2000, respectively. Next CNTs with 0.15 mg/mL were added into the pNIPAM solution. Before ultraviolet (UV) curing, N_2 gas was bubbled for 15 min to remove oxygen from the mixed solution. After dipping the pNIPAM solution over the PET film covered with an acrylic plastic chamber to define the shape (22 mm long, 7.5−20 mm wide, and 1 mm high), 365 nm UV exposure at a 6 W power was applied for 15 (10) min for pNIPAM without (with) CNTs. This difference in exposure time is based on our experience. Finally, a pNIPAM film with water on a PET film was packaged by a polyvinylidene chloride (PVDC) film (10.5 μm thick). To seal completely, the edge of the PVDC (~2 mm wide) was heated at ~140 °C. Figure 1c shows the fabricated pNIPAM actuators with and without CNTs.

RESULTS AND DISCUSSION

Figure 1d depicts the actuation mechanism when pNIPAM is placed onto a PET film. Above 32 °C, pNIPAM starts to release water, causing it to shrink. However, the small temperature difference between room temperature and 32 °C has a negligible effect on the shape of the PET film. Because of the bilayer structure, the device bends because pNIPAM generates a compressive force. Although there is PVDC film packaging surrounding the bilayer structure, the device can bend if the PVDC film is soft enough that the force from the bilayer structure actuation bends it. When pNIPAMs with or without CNTs is placed on a hot plate at 50 °C, the actuator bends (Figure 2a,b).

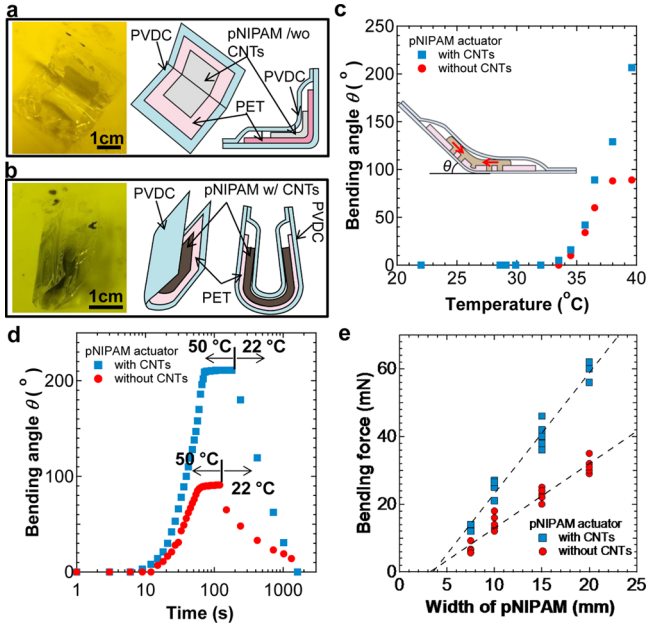

Figure 2. Characteristics of the pNIPAM actuator stimulated by temperature. Photos and schematics of the pNIPAM actuator on a hot plate set at 50 °C (a) without and (b) with CNTs. (c) Bending angle of the actuators as a function of hot plate temperature. (d) Response times of the pNIPAM actuator at 50 and 22 °C. (e) Bending force as a function of the width of pNIPAM with and without CNTs.

To understand the packaged pNIPAM properties, the fundamental actuations of pNIPAM with and without CNTs were characterized. Figure 2c plots the bending angle response

DOI: 10.1021/acsami.5b02544
ACS Appl. Mater. Interfaces 2015, 7, 11002−11006

as a function of the stage (hot plate) temperature where the actuator is placed. The bending angle is determined by the line fitting on the both edges of the pNIPAM actuators as described in Supporting Information, Figure S1. Because the LCST of pNIPAM is ~32 °C, the pNIPAM actuator starts to bend at ~33.5 °C and has a linear dependence of ~23.8°/°C between 33.5 and 38 °C. The actuated angle measurements were conducted in an air-conditioned room, resulting in a transition that spans a wide range due to the temperature difference between pNIPAM on the bottom surface (i.e., a hot plate contact) and the top surface (i.e., air ambient at ~22 °C) with and without CNTs. Above 38 °C, the bending angle reaches ~90° (210°) without (with) CNTs. As discussed in detail below, the large difference in the maximum bending angle with and without CNTs is most likely due to the adhesion between the PET film and pNIPAM in the presence or absence of CNTs.

Next the response speed of the actuator stimulated by temperature was characterized. pNIPAM was placed on a hot plate set at 50 °C, and the bending angle was measured as a function of time. Figure 2d suggests that the response times of the pNIPAM actuator without CNTs are ~80 s and >20 min to reach the maximum bending angle (~90°) and to restore the flat state, respectively. In contrast, pNIPAM with CNTs realizes response times of ~72 s and ~12 min to reach the maximum angle of ~210° and to return to the flat state, respectively. The fact that the bending angle more than doubles for pNIPAM with CNTs (~210°) compared to that without CNTs (~90°) suggests that adding CNTs inside a pNIPAM film drastically improves the response time. This improvement is mostly due to the high thermal conductivity (~3500 W m^{-1} K^{-1})[21] of CNTs, which increases the responses to the thermal stimulus from the hot plate and the ambient temperature. In fact, Supporting Information, Figure S2 shows that the temperature difference is ~0.9 °C between pNIPAM with and without CNTs on a hot plate. The plateau of bending angle at ~70 s in Figure 2d means that the actuator reaches the maximum bending angles. Regardless of the CNT content in pNIPAM, this is the first demonstration of a pNIPAM actuator with a packaging technique operated in ambient air.

The actuation force is another important factor when designing applications using this packaging technique. Figure 2e (Supporting Information, Figure S3) plots the actuation force as a function of the width (W) of pNIPAM at a constant length (L) of 22 mm. The linear fit of the force strength with CNTs (without CNTs) by width is ~3.6 mN/mm (~1.9 mN/mm), indicating that the threshold width (W) to bend the actuator is ~3.5 mm (~3.2 mm) because the pNIPAM force must overcome the force of the packaging edge to be flat. It is noteworthy that the pNIPAM actuator with CNTs has roughly double the force (~42 mN) with W = 15 mm (Figure 2e), which agrees well with the actuation bending angle. These results indicate that the force of the pNIPAM-based actuator can be experimentally measured in ambient air.

Then, the repeatability of the pNIPAM actuator (W = 15 mm and L = 22 mm) was evaluated. Samples without and with CNTs were kept in ambient air at 18.3 °C and 25.7% humidity. Figure 3a shows the actuation bending angle change, $\Delta\theta$ (= $\theta - \theta_0)/\theta_0$, as a function of the actuation cycle, where θ_0 and θ are the first measured and each cycle angle at 50 °C, respectively. The bending angle of the actuator without CNTs degrades at a rate of 2.2%/cycle, while that with CNTs does not. There are two possible reasons for the degradation without CNTs: water

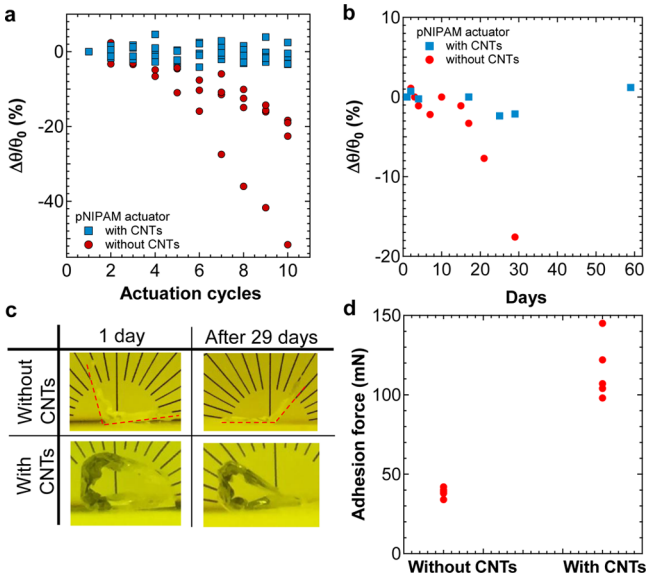

Figure 3. Actuation reliability. (a) Normalized bending angle change, $\Delta\theta/\theta_0$, as a function of the actuation cycle. (b) Normalized bending angle change as a function of time (in d). (c) Photos of the pNIPAM actuators with and without CNTs at 50 °C as fabricated (1 d) and 29 d after fabrication. (d) Adhesion force between the PET film and the pNIPAM film with and without CNTs.

evaporation from pNIPAM through the PVDC film and poor adhesion and delamination of the pNIPAM film from the PET film. The poor repeatability is mostly due to the adhesion between pNIPAM and PET because the stability in the bending angle with CNTs suggests that water does not evaporate through the PVDC packaging film. Furthermore, pNIPAM with CNTs has a better repeatability for frequent time usage.

The time dependence of the device performance is another important factor for practical applications. Figure 3b,c depicts the normalized bending angle change as a function of time up to 59 d and photos of actuators on a hot plate at 50 °C after 1 d and 29 d, respectively. After 59 d, the bending angle for the actuator with CNTs does not change. PVDC is not a perfect blocking layer for water vapor permeability, although it has a 10−100 smaller water permeability constant (~0.2 × 10^8 at 25 °C)[22] than other polymer films. Therefore, water may gradually evaporate through a PDVC film. If water vapor evaporation must be prevented, the packaging film must have a high water-blocking layer such as an ultrathin glass film and Al_2O_3 layer coating film.[23] For the actuator without CNTs, the trend of degradation is similar to the results of cycle test shown in Figure 3a regardless of the number of days due to the poor reliability of the bending cycle. The results confirm that the actuator with CNTs shows good repeatability and reliability without degradation for at least 60 d.

To analyze the bending angle and reliability differences between the actuators with and without CNTs, the adhesion between a pNIPAM film and a PET substrate was checked by mechanical peeling of the pNIPAM film from the PET. Interestingly, the pNIPAM film with CNTs has adhesion with an average peeling force of 115.2 mN. This value is ~3 times stronger than that without CNTs, which has an average peeling force of 38.6 mN. Comparing the bending forces to the adhesion force for pNIPAM without CNTs (Figure 2e vs Figure 3d), the values are similar but the bending force is slightly higher. We envision that when pNIPAM without CNTs

DOI: 10.1021/acsami.5b02544
ACS Appl. Mater. Interfaces 2015, 7, 11002−11006

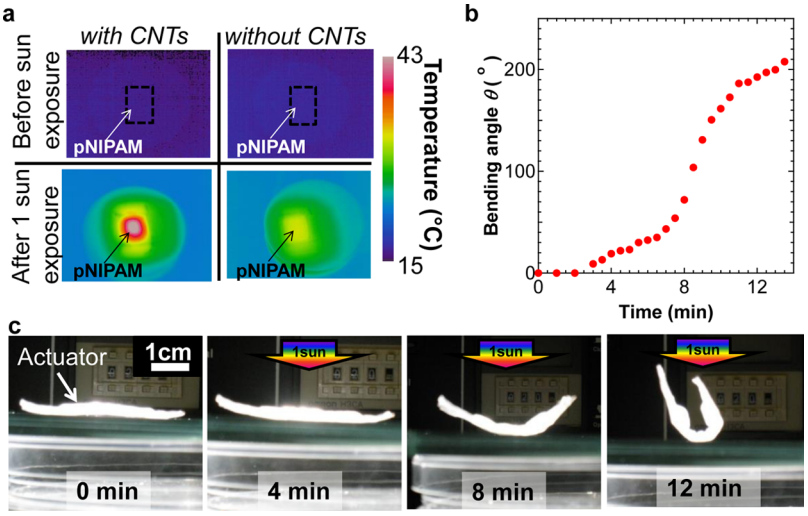

Figure 4. Sunlight-stimulating pNIPAM actuator. (a) Temperature distributions under 100 mW/cm^2 (one sun) for pNIPAM actuators with and without CNTs measured by an infrared camera. (b) Bending angle under one sun as a function of exposure time. (c) Photos of the pNIPAM actuator with CNTs under one sun at 0, 4, 8, and 12 min.

is bent, the force is also applied to the delamination of the pNIPAM film from the PET film, causing the pNIPAM actuator, especially the interface between pNIPAM and PET, to become damaged, directly affecting the degradation of the bending angle during the multiple cycle test (Figure 3a). This adhesion difference creates a bending angle difference mostly because the strain caused by pNIPAM film regardless of CNT concentration (0 mg/mL (i.e., without CNTs) to 1 mg/mL) in pNIPAM is almost same as previously reported.[16] Furthermore, this also affects the cycle repeatability, which is consistent with the experimental results shown in Figure 3a.

Next, the optical responsiveness was analyzed using a solar simulator (XES-40S2-CE, San-ei Electric) to generate 100 mW/cm^2 (one sun). Sunlight is converted into temperature by absorbing mainly infrared light. The temperature distributions for pNIPAM actuators with and without CNTs were observed using an infrared camera before and after exposure to one sun (Figure 4a and Supporting Information, Figure S4). Regardless of the presence of CNTs, the temperature increases upon exposure to one sun; because of the CNT's ability to absorb light, pNIPAM with CNTs reaches the LCST of 32 °C within 3 min, whereas that without CNTs does not reach the LCST even after 10 min (31.7 °C).

The response time of a pNIPAM actuator with CNTs was characterized by measuring the bending angle (Figure 4b,c). In ~3 min, the actuator starts to bend (surface temperature of ~34 °C), and the angle gradually increases to 210° in 14 min. A step in the bending angle occurs between 4 and 8 min (Figure 4b), which is attributed to an angle change because the light exposure area or direction affects the heating speed of pNIPAM upon exposure to one sun. The energy conversion efficiency is estimated by extracting the strain energy density under one sun exposure. To simplify the calculation, bilayer structure (i.e., pNIPAM/PET) was used to approximate the strain energy density.[1,24] In 8 min of exposure, the deflection of pNIPAM actuator is ~1.9 cm that corresponds to the energy of ~0.026 J. By comparing the sunlight energy exposed for 8 min (~323 J), the energy conversion efficiency is ~0.008%. Although it takes a relatively long time (14 min) to reach the maximum bending angle (~210°) and low efficiency, sunlight can successfully operate pNIPAM with CNTs.

Finally, as proofs-of-concept, two types of applications are demonstrated using natural power sources. The first application is a wearable device that can conformally cover skin using heat from the human body. Figure 5a indicates that pNIPAM with CNTs can bend and cover a human finger upon being actuated by the temperature of a human body (~32−33 °C). The next application utilizes sunlight as the power source. By forming

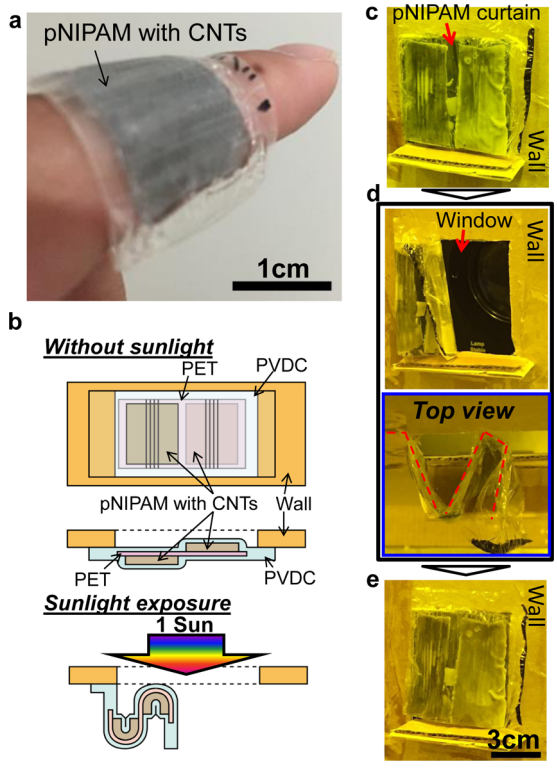

Figure 5. Demonstrations of the pNIPAM actuators stimulated by the human skin temperature and sunlight. (a) Wearable sheet actuated by skin temperature wraps around a finger. (b) Schematic of the smart curtain design. Photos of an electrically powerless smart curtain (c) before sunlight exposure (closed), (d) after exposure for 15 min (open), and (e) after terminating sunlight exposure (closed).

DOI: 10.1021/acsami.5b02544
ACS Appl. Mater. Interfaces 2015, 7, 11002−11006

pNIPAM films on both sides of a PET film at different positions (Figure 5b), an electrically powerless sunlight-operated curtain is demonstrated. Because of shrinkage of pNIPAM, the bending directions can be controlled by designing the pNIPMA either on the top or bottom surface of the substrate. A pNIPAM smart curtain was set on a wall with a square hole as a window (Figure 5c). Exposing the small curtain to sunlight causes it to open (Figure 5d), while terminating exposure (i.e., at night) causes it to close (Figure 5e) (Supplementary Information, video). Although here we only demonstrate a smart curtain, this concept may be applied to the joints of robots, allowing operations by sunlight without using artificial electrical power. Since sunlight is required to actuate, the applications are limited. Because this is only the first step of the demonstration, further development should open a new class of electrical powerless device.

CONCLUSION

In conclusion, we propose an electrically powerless thermal- and light-responsive pNIPAM actuator in ambient air using a packaging technique. In particular, this actuator can be operated by stimuli of the temperature of the human body and sunlight without another artificial power source. This natural power source actuator can be used for a wearable device that wraps around a human body, a smart wall/curtain that opens and closes by sunlight, etc. These proofs-of-concept are demonstrated to show the potential applications toward powerless, solid−liquid composite device platforms. A natural power source actuator should lead to the next generation of ultimate low-power devices.

ASSOCIATED CONTENT

Supporting Information

Temperature distribution of pNIPAM with and without CNTs on a hoplate and under sunlight, response of pNIPAM actuator with different width of pNIPAM, bending angle of pNIPAM, movie clips of a proof-of-concept of a smart curtain. The Supporting Information is available free of charge on the ACS Publications website at DOI: 10.1021/acsami.5b02544.

AUTHOR INFORMATION

Corresponding Author

*E-mail: takei@pe.osakafu-u.ac.jp.

Notes

The authors declare no competing financial interest.

ACKNOWLEDGMENTS

This work was partially supported by JSPS KAKENHI Grant Nos. 26630164 and 26709026 and by the Asahi Glass Foundation.

REFERENCES

(1) Zhang, X.; Yu, Z.; Wang, C.; Zarrouk, D.; Seo, J. W.; Cheng, J. C.; Buchan, A. D.; Takei, K.; Zhao, Y.; Ager, J. W.; Zhang, J.; Hettick, M.; Hersam, M. C.; Pisano, A. P.; Fearing, R. S.; Javey, A. Photoactuators and Motors Based on Carbon Nanotubes with Selective Chirality Distributions. *Nat. Commun.* **2014**, *5*, 2983.

(2) Ahir, S. V.; Terentjev, E. M. Photomechanical Actuation in Polymer-Nanotube Composites. *Nat. Mater.* **2005**, *4*, 491−495.

(3) Wu, C.; Feng, J.; Peng, L.; Ni, Y.; Liang, H.; He, L.; Xie, Y. Large-Area Graphene Realizing Ultrasensitive Photothermal Actuator with High Transparency: New Prototype Robotic Motions Under Infrared-Light Stimuli. *J. Mater. Chem.* **2011**, *21*, 18584−18591.

(4) Park, S.; An, J.; Suk, J. W.; Ruoff, R. S. Graphene-Based Actuators. *Small* **2010**, *6*, 210−212.

(5) Liang, J.; Xu, Y.; Huang, Y.; Zhang, L.; Wang, Y.; Ma, Y.; Li, F.; Guo, T.; Chen, Y. Infrared-Triggered Actuators from Graphene-Based Nanocomposites. *J. Phys. Chem. C* **2009**, *113*, 9921−9927.

(6) Wang, E.; Desai, M. S.; Lee, S. W. Light-Controlled Graphene-Elastin Composite Hydrogel Actuators. *Nano Lett.* **2013**, *13*, 2826−2830.

(7) Kam, N. W.; O'Connell, M.; Wisdom, J. A.; Dai, H. Carbon Nanotubes as Multifunctional Biological Transporters and Near-Infrared Agents for Selective Cancer Cell Destruction. *Proc. Natl. Acad. Sci. U. S. A.* **2005**, *102*, 11600−11605.

(8) Kobatake, S.; Takami, S.; Muto, H.; Ishikawa, T.; Irie, M. Rapid and Reversible Shape Changes of Molecular Crystals on Photoirradiation. *Nature* **2007**, *446*, 778−781.

(9) Yu, Y.; Nakano, M.; Ikeda, T. Directed Bending of a Polymer Film by Light. *Nature* **2003**, *425*, 145.

(10) Barrett, C. J.; Mamiya, J.-i.; Yager, K. G.; Ikeda, T. Photo-Mechanical Effects in Azobenzene-Containing Soft Materials. *Soft Matter* **2007**, *3*, 1249−1261.

(11) Takashima, Y.; Hatanaka, S.; Otsubo, M.; Nakahata, M.; Kakuta, T.; Hashidzume, A.; Yamaguchi, H.; Harada, A. Expansion-Contraction of Photoresponsive Artificial Muscle Regulated by Host-Guest Interactions. *Nat. Commun.* **2012**, *3*, 1270.

(12) Lan, T.; Hu, Y.; Wu, G.; Tao, X.; Chen, W. Wavelength-Selective and Rebound-able Bimorph Photoactuator Driven by a Dynamic Mass Transport Process. *J. Mater. Chem. C* **2015**, *3*, 1888−1892.

(13) Liu, K.; Cheng, C.; Cheng, Z.; Wang, K.; Ramesh, R.; Wu, J. Giant-Amplitude, High-Work Density Microactuators with Phase Transition Activated Nanolayer Bimorphs. *Nano Lett.* **2012**, *12*, 6302−6308.

(14) Stuart, M. A.; Huck, W. T.; Genzer, J.; Muller, M.; Ober, C.; Stamm, M.; Sukhorukov, G. B.; Szleifer, I.; Tsukruk, V. V.; Urban, M.; Winnik, F.; Zauscher, S.; Luzinov, I.; Minko, S. Emerging Applications of Stimuli-Responsive Polymer Materials. *Nat. Mater.* **2010**, *9*, 101−113.

(15) Lendlein, A.; Kelch, S. Shape-Memory Polymers. *Angew. Chem., Int. Ed.* **2002**, *41*, 2034−2057.

(16) Zhang, X.; Pint, C. L.; Lee, M. H.; Schubert, B. E.; Jamshidi, A.; Takei, K.; Ko, H.; Gillies, A.; Bardhan, R.; Urban, J. J.; Wu, M.; Fearing, R.; Javey, A. Optically- and Thermally-Responsive Programmable Materials Based on Carbon Nanotube-Hydrogel Polymer Composites. *Nano Lett.* **2011**, *11*, 3239−3244.

(17) Schild, H. G. Poly(N-Isopropylacrylamide): Experiment, Theory and Application. *Prog. Polym. Sci.* **1992**, *17*, 163−249.

(18) Ko, H.; Zhang, Z.; Chueh, Y. L.; Saiz, E.; Javey, A. Thermoresponsive Chemical Connectors Based on Hybrid Nanowire Forests. *Angew. Chem., Int. Ed.* **2010**, *49*, 616−619.

(19) Ota, H.; Chen, K.; Lin, Y.; Kiriya, D.; Shiraki, H.; Yu, Z.; Ha, T. J.; Javey, A. Highly Deformable Liquid-State Heterojunction Sensors. *Nat. Commun.* **2014**, *5*, 5032.

(20) Park, Y.-L.; Chen, B.-R.; Wood, R. J. Design and Fabrication of Soft Artificial Skin Using Embedded Microchannels and Liquid Conductors. *IEEE Sens. J.* **2012**, *12*, 2711−2718.

(21) E, P.; Mann, D.; Wang, Q.; Goodson, K.; Dai, H. Thermal Conductance of an Individual Single-Wall Carbon Nanotube above Room Temperature. *Nano Lett.* **2006**, *6*, 96−100.

(22) Doty, P. M.; Aiken, W. H.; Mark, H. Temperature Dependence of Water Vapor Permeability. *Ind. Eng. Chem.* **1946**, *38*, 788−791.

(23) Carcia, P. F.; McLean, R. S.; Reilly, M. H.; Groner, M. D.; George, S. M. Ca Test of Al_2O_3 Gas Diffusion Barriers Grown by Atomic Layer Deposition on Polymers. *Appl. Phys. Lett.* **2006**, *89*, 031915.

(24) Merced, E.; Tan, X.; Sepúlveda, N. Strain Energy Density of VO_2-Based Microactuators. *Sens. Actuators, A* **2013**, *196*, 30−37.

DOI: 10.1021/acsami.5b02544
ACS Appl. Mater. Interfaces 2015, 7, 11002−11006